J. Condensed Matter Nucl. Sci. 17 (2015) 67–90

Research Article

O-site and T-site Occupation of α-phase PdH_x and PdD_x

Peter L. Hagelstein*

Massachusetts Institute of Technology, Cambridge, MA 02139, USA

Abstract

An important study of the solubility of hydrogen in α-phase PdH_x and deuterium in α-phase PdD_x over a wide temperature range was published by Clewley et al. (*J. Chem. Soc., Faraday Trans. 1: Phy. Chem. Condensed Phases* **69** (1973) 449–458). An analysis of the data based on an empirical solubility model based on O-site occupation allows for an understanding of the data at low temperature, but probably is not a good starting place for understanding the solubility at high temperature. We have applied a recently developed empirical model for both O-site and T-site occupation to this data set, and find good agreement between data and a basic version of the model which assumes that the O-site and T-site partition functions are taken to be harmonic oscillator partition functions. Even better agreement is obtained when a more realistic O-site partition function is used. A range of optimum models with different assumptions about the T-site partition function is considered, and it is found to be possible to select one that matches the T-site occupation at zero loading inferred from neutron diffraction measurements of Pitt and Gray (*Europhys. Let.* **64** (2003) 344). The O-site to T-site excitation energy is assumed independent of temperature in these models, and we obtain specific model values of 105.3 meV for α-phase PdD_x and 106.5 meV for α-phase PdH_x.
 ISSN 2227-3123

Keywords: Empirical model, Mean-field lattice gas model, Solubility, α-phase PdH_x and PdD_x, Tetrahedral occupation

1. Introduction

Even though palladium hydride has been studied for almost a century and a half [1–12], there remains much that we do not know about some very basic issues. For example, interstitial hydrogen is known to occupy octahedral sites in bulk FCC palladium hydride, but it has not been established experimentally where additional hydrogen might go under high loading conditions where all of the O-sites are occupied (see Ref. [13] and references therein). Recent calculations of the O-site to T-site excitation energy indicate that the energy might be sufficiently low [14–20] that one could reasonably expect that there would be a small but observable T-site occupation at elevated temperature. In this work we propose to study this issue by comparing an appropriate model for O-site and T-site occupation with an old but important experimental data set for α-phase PdH_x and PdD_x [21]. We are able to extract plausible values for the O-site to T-site excitation energy from this comparison, which are generally consistent with the recent calculations.

*E-mail: plh@mit.edu

 ISSN 2227-3123

The experimental data consists of low pressure solubility data for α-phase PdH_x and PdD_x, where the interstitial hydrogen and deuterium concentration is low. Early theoretical models relevant to this regime were studied by Fowler [22] and Lacher [23]. Subsequent modeling of solubility at both low and high pressure has been reported by many authors [24–33]. Hydrogen and deuterium solubility has been studied in many experimental works [34–52]. To our knowledge there has not been an earlier study of α-phase PdH_x or PdD_x in which T-site occupation was modeled and a comparison with experimental data reported.

To carry out such an analysis, we can make use of a model for interstitial O-site and T-site occupation that was recently used to model PdD and PdH at high loading [13]. In a sense this kind of model is at the same time very simple and very powerful; following the early work of Fowler [22] and of Lacher [23] we assume equilibrium between H_2 (or D_2) in the gas phase and interstitial H (or D) which can occupy O-sites, and now also T-sites. An equilibrium statistical mechanics model requires a knowledge of the energy levels in the gas and the solid, and also a knowledge of the various partition functions associated with both phases. Over the years most of the relevant pieces of the model that we need have been studied, so that for us the largest uncertainty is in the O-site to T-site excitation energy and T-site partition functions It is possible to develop an estimate for the excitation energy and assess model partition functions by optimizing the empirical model to the experimental data set.

While simple in concept, it has become clear through working with the model and data that there are many issues. If we compare the most basic version of the model based on 3D simple harmonic partition functions, then we obtain rather good fits of the experimental data, and we obtain estimates for the excitation energy in line with recent calculations. If we work with more sophisticated partition function models, then we can get a range of excitation energies depending on the details of the models. If we accept results from neutron diffraction experiments, then we can identify a specific partition function model for PdD_x which is at the same time a good fit for the solubility data and is also consistent with the neutron diffraction data.

2. O-site Occupation and α-phase PdH_x and PdD_x Data

Hydrogen and deuterium solubility in Pd in the α-phase was studied experimentally by Clewley et al. [21], where data was reported for a wide range of temperatures from below 200 K to more than 1200 K. In this section we consider a simple analysis of the data based on a picture in which the interstitial hydrogen or deuterium is restricted to octahedral sites. If tetrahedral site occupation were to occur, one might expect that it should impact the analysis only at elevated temperature since the O-site to T-site excitation energy is expect to be on the order of 100–300 meV. Consequently we expect an analysis carried out assuming only O-site excitation should give reliable results in the low temperature regime.

2.1. Equilibrium between gas phase and solid phase deuterium

It is possible to develop a model for O-site occupation of deuterium starting from a picture in which gas phase D_2 is in equilibrium with solid phase interstitial deuterium in palladium. Under these conditions the chemical potential of deuterium in the two phases are equal [24,39]

$$\mu_{\rm D}^{\rm (s)} = \mu_{\rm D}^{\rm (g)} = \frac{1}{2}\mu_{\rm D_2}. \tag{1}$$

This is equivalent to the equilibrium constraints worked with by Fowler [22] and by Lacher [23].

2.2. Gas phase chemical potential

The chemical potential of deuterium in gas phase D_2 is well known, and can be written as [32,53]

$$\mu_{D_2} = -E_D + \mu_{\text{nonideal}} - k_B T \ln z_{\text{rot}}. \tag{2}$$

Here E_D is the dissociation energy [54]

$$E_D\ [H_2] = 4.4780\ \text{eV}, \tag{3}$$

$$E_D\ [D_2] = 4.5561\ \text{eV}. \tag{4}$$

The nonideal gas contribution to the chemical potential is

$$\mu_{\text{nonideal}} = k_B T \ln \left[\frac{f}{k_B T} \left(\frac{2\pi\hbar^2}{M k_B T} \right)^{3/2} \right], \tag{5}$$

where f is the fugacity and M is the mass of the molecule. For the fugacity of H_2 and of D_2 we make use of the model for H_2 of Joubert [55]; in the low pressure regime the fugacity is well approximated by the pressure. For the rotational partition function we use [56]

$$\text{PdH} : z_{\text{rot}} = 1 \sum_{\text{even } l} \sum_n (2l+1)\ \mathrm{e}^{-E_{\text{nl}}/k_B T} + 3 \sum_{\text{odd } l} \sum_n (2l+1)\ \mathrm{e}^{-E_{\text{nl}}/k_B T}, \tag{6}$$

$$\text{PdD} : z_{\text{rot}} = 6 \sum_{\text{even } l} \sum_n (2l+1)\ \mathrm{e}^{-E_{\text{nl}}/k_B T} + 3 \sum_{\text{odd } l} \sum_n (2l+1)\ \mathrm{e}^{-E_{\text{nl}}/k_B T}. \tag{7}$$

These partition functions includes the nuclear spin degeneracy explicitly. For the molecular energy levels E_{nl} we made use of the fits of Urey and Rittenberg [57].

At the temperatures of interest we do not expect electronic excitation, so the electronic degeneracy is 1; in this case

$$\mu_e = -k_B T \ln z_e = 0, \tag{8}$$

so there is no electronic contribution to the gas phase chemical potential. We neglect molecular dissociation.

2.3. Solid phase chemical potential

For solid phase interstitial deuterium we can write [32,13]

$$\mu_D = E_O + \theta_O \frac{\partial E_O}{\partial \theta} - k_B T \ln \frac{1-\theta_O}{\theta_O} - k_B T \ln z_O, \tag{9}$$

where E_O is the O-site energy, which in general depends on the temperature and on the D/Pd loading. The O-site fractional occupation is θ_O (which is the ratio of the number of interstitial O-site deuterium atoms to the number of Pd atoms). We take the partition function of an occupied O-site to be

$$z_O\ [\text{PdH}] = 4 \left(\frac{1}{1 - \mathrm{e}^{-\hbar\omega_O[\text{PdH}]/k_B T}} \right)^3, \tag{10}$$

$$z_{\rm O}\ [{\rm PdD}] = 6\left(\frac{1}{1-\ {\rm e}^{-\hbar\omega_{\rm O}[{\rm PdD}]/k_{\rm B}T}}\right)^3. \tag{11}$$

Normally this partition function is that of a three-dimensional harmonic oscillator [25] referenced to the potential minimum [30,32]; here we take the reference energy of the O-site to include the zero-point contribution. The spin 1/2 proton degeneracy is 2; the deuteron spin degeneracy is 3; and the electronic spin degeneracy is 2. The O-sites are modeled as oscillators with energies [58]

$$\hbar\omega_{\rm O}\ [{\rm PdH}] = 69.0\ {\rm meV}, \tag{12}$$

$$\hbar\omega_{\rm O}\ [{\rm PdD}] = 46.5\ {\rm meV}. \tag{13}$$

2.4. Analysis of the O-site energy

It is possible to develop an estimate for the O-site energy in the limit of zero loading (at low temperature) from experimental data. To do so, we rearrange Eq. (9) according to

$$E_{\rm O} + \theta_{\rm O}\frac{\partial E_{\rm O}}{\partial\theta} = \mu_{\rm D} + k_{\rm B}T\ln\frac{1-\theta_{\rm O}}{\theta_{\rm O}} + k_{\rm B}T\ln z_{\rm O}. \tag{14}$$

At sufficiently low loading the linear term of the left hand side becomes sufficiently small that it can be neglected, so we may write

$$E_{\rm O}(\theta\to 0)\ \to\ \mu_{\rm D} + k_{\rm B}T\ln\frac{1-\theta_{\rm O}}{\theta_{\rm O}} + k_{\rm B}T\ln z_{\rm O}. \tag{15}$$

In general the loading fraction θ is made up of O-site and T-site contributions ($\theta_{\rm O}$ and $\theta_{\rm T}$); if there were no T-site occupation then $\theta\to\theta_{\rm O}$).

In Clewley et al. [21] data is presented for the parameter

$$p\frac{(1-\theta)^2}{\theta^2}. \tag{16}$$

as a function of $1/T$. At low pressure the loading becomes sufficiently small that the estimate above for the O-site energy at zero loading above becomes accurate. Hence we can work with the experimentally observed solubility data to infer a value of $E_{\rm O}(\theta\to 0)$ for each data point based on

$$E_{\rm O}(\theta\to 0)\ \to\ \mu_{\rm D} + k_{\rm B}T\ln\frac{1-\theta}{\theta} + k_{\rm B}T\ln z_{\rm O}. \tag{17}$$

In the experimental data there could be both O-site and T-site contributions to θ; so in writing this we propose to infer the O-site energy from data that may have both O-site and T-site contributions. The results are plotted as a function of T in Fig. 1. One observes that the data points are roughly linear at low temperature; but once the temperature rises above about 400 K the dependence of this parameter deviates considerably from its low temperature behavior. This deviation from linearity for us is an indication that new physics might be present.

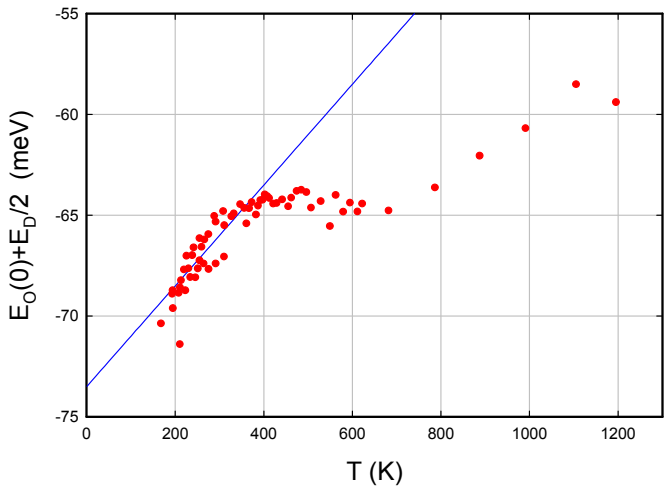

Figure 1. O-site energy at zero loading for α-phase PdD_x as a function of temperature estimated from the data of Clewley et al. [21] (red circles); linear fit to the data at low temperature (blue line).

2.5. Fermi level as a function of temperature

The increase in the O-site energy in the low temperature regime may be related to the change in the Fermi level with temperature. We recall that the Fermi level in a metal is determined by the charge neutrality constraint [56]

$$n_e = \int g(\epsilon) \frac{1}{1 + e^{(\epsilon-\mu_F)/k_B T}} d\epsilon, \tag{18}$$

where $g(\epsilon)$ is the density of states per unit volume and μ_F is the Fermi level. We have worked with the density of states of Mueller et al. [59] shown in Fig. 2. The resulting incremental Fermi level is shown in Fig. 3. This result is in good agreement with a similar computation of Fradin [60].

We have fit the incremental Fermi level as a function of T according to

$$\begin{aligned} \Delta\mu_F(T) &= \mu_F(T) - \mu_F(0) \\ &= a_0 + a_1 T + a_2 T^2 + a_3 T^3 + a_4 T^4 + a_5 T^5 + a_6 T^6 \end{aligned} \tag{19}$$

with T in Kelvin and with fitting coefficients given by

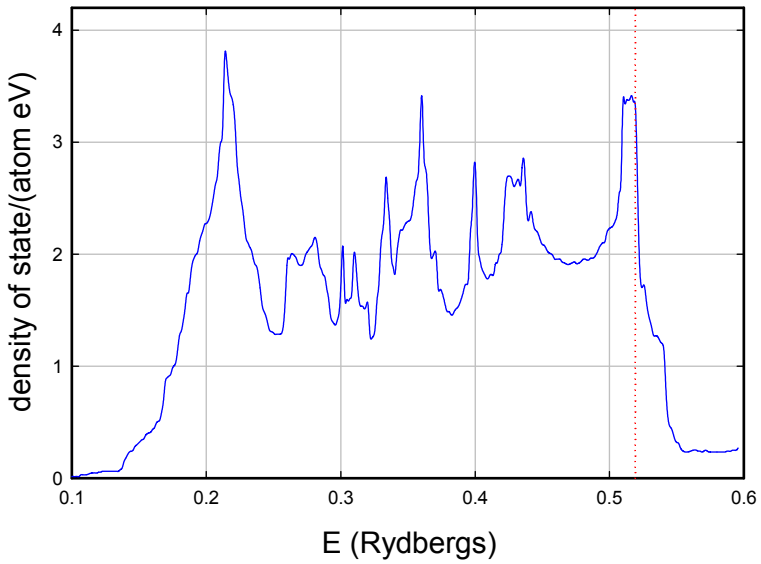

Figure 2. Density of state per unit volume for Pd from Mueller et al. [59] (blue line); Fermi level at $T = 0$ (red dotted line).

$$\begin{aligned}
a_0 &= 0.106352,\\
a_1 &= -0.0055007,\\
a_2 &= 0.000108379,\\
a_3 &= -1.53795 \times 10^{-7},\\
a_4 &= 1.24472 \times 10^{-10},\\
a_5 &= -5.12753 \times 10^{-14},\\
a_6 &= 8.53854 \times 10^{-18}.
\end{aligned} \tag{20}$$

2.6. Comparison of the O-site energy with data

We suspect that at low temperature the increase in the O-site energy at zero loading is dominated by the contribution of the incremental Fermi level. To pursue this we plot a shifted version of the data for both α-phase PdH_x and PdD_x with the incremental Fermi level in Fig. 4. Although there is much scatter in the data plotted this way, we conclude that there is a consistency between the electronic Fermi level shift and the O-site energies estimated from the data of Clewley et al. [21] below about 350 K.

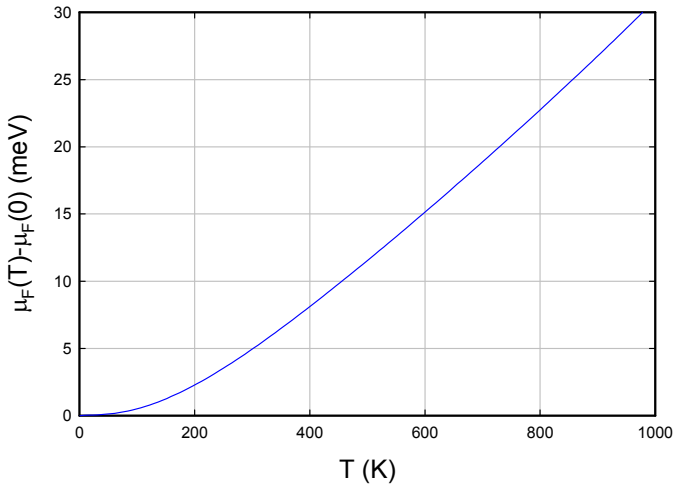

Figure 3. Incremental Fermi level for Pd as a function of temperature.

2.7. Interstitial partition function

Another interpretation of the data is possible, one which focuses on the partition function of interstitial hydrogen or deuterium. If we presume that the O-site energy is given by

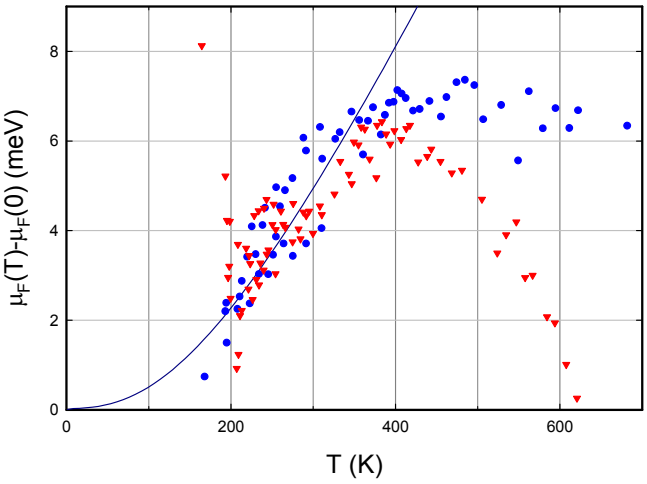

Figure 4. Shifted O-site energies for α-phase PdD_x (blue circles) and α-phase PdH_x (red triangles) as a function of temperature; also, incremental Fermi level (dark blue line) plotted as a function of temperature.

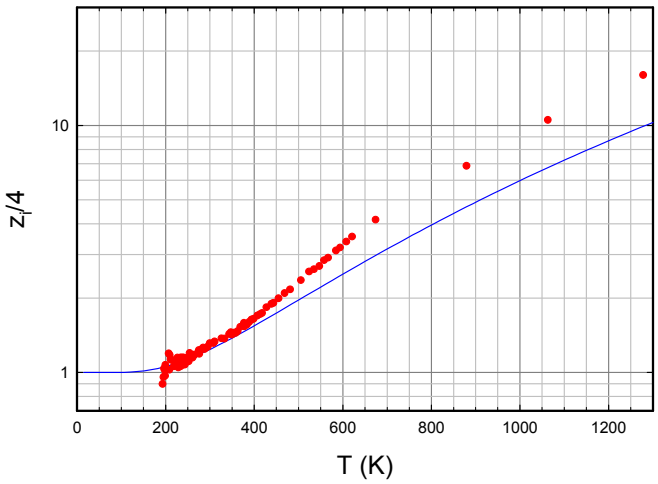

Figure 5. Scaled interstitial partition function as a function of temperature; experimental data of Clewley et al. for PdH_x represented as a scaled interstitial partition function as described in the text (red circles); analogous O-site partition function for a three-dimension simple harmonic oscillator (blue line).

$$E_{\rm O}(T) = E_{\rm O}(0) + \Delta\mu_{\rm F}(T) \tag{21}$$

as an ansatz, then we would be able to determine the partition function of the interstitials according to

$$z_{\rm i} = \left(\frac{\theta}{1-\theta}\right) \exp\left\{\frac{E_{\rm O}(0) + \Delta\mu_{\rm F}(T) - \mu_{\rm D}}{k_{\rm B}T}\right\}. \tag{22}$$

The idea here is that the θ from the experimental data may have both O-site and T-site contributions; we would use $z_{\rm O}$ for the O-site partition function, and $z_{\rm T}$ for the T-site partition function. In this equation $z_{\rm i}$ is the partition function of interstitial hydrogen or deuterium under conditions where both O-site and T-site occupation may be present. In this case we have experimental data points for θ at different temperatures, and if we assume a pressure then we can determine a corresponding value for the chemical potential. We can choose a value for $E_{\rm O}(0)$ to match the data at $T = 0$ so that $z_{\rm i}(0)$ goes to the appropriate statistical factor due to electronic and nuclear spin contributions.

In Fig. 5 is shown results for the data of Clewley et al. [21] for α-phase PdH_x analyzed in terms of the equivalent (and scaled) interstitial partition function, along with the analogous O-site partition function based on a 3D harmonic oscillator. The O-site energy at zero temperature for this plot is

$$E_{\rm O}(0) = -\frac{E_{\rm D}}{2} - 75.5 \text{ meV}. \tag{23}$$

The data plotted this way is interesting for a number of reasons. One is that at low temperature there is pretty good agreement, suggesting that the basic approach seems sound. And independent of any additional assumptions, if the O-site energy depends on temperature as in our ansatz, then the resulting partition function is already not too far from

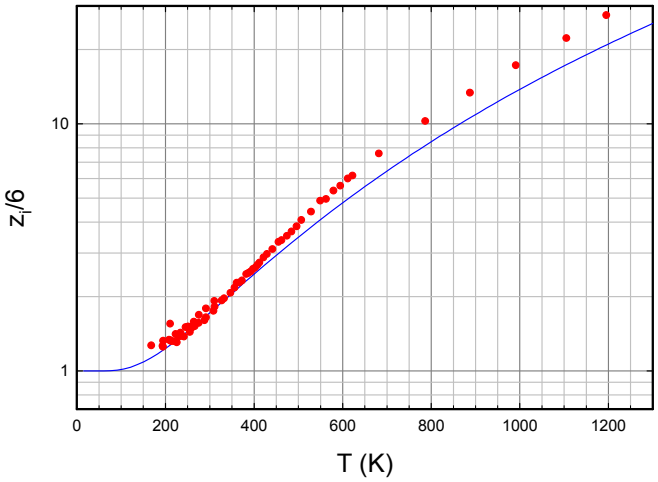

Figure 6. Scaled interstitial partition function as a function of temperature; experimental data of Clewley et al. for PdD_x represented as a scaled interstitial partition function as described in the text (red circles); analogous O-site partition function for a three-dimension simple harmonic oscillator (blue line).

that of a 3D harmonic oscillator over the entire temperature range. This is significant, as one would compute a very different partition function based on an embedded atom model potential, or based on the approach of Sazonov et al. [61].

The data plotted similarly for α-phase PdD_x is shown in Fig. 6. In this case the O-site energy at zero temperature is

$$E_O(0) = -\frac{E_D}{2} - 70.3 \text{ meV}. \tag{24}$$

Qualitatively the situation is very similar, except that in this case the deviation from the partition function of a 3D oscillator seems smaller (since the 3D oscillator partition function is larger in magnitude).

2.8. Discussion

One expects to be able to understand the solubility of hydrogen and deuterium in the α-phase at low temperature based on a simple picture with O-site occupation, and it is comforting that there is a reasonably good match between data and model in this regime. It would be possible to fit to a linear empirical model for the O-site energy; however, it is much more satisfying that the slope might be accounted for by the temperature dependence of the Fermi level.

It seems clear that this simple picture is not going to extend into the higher temperature regime without some modification. For both hydrogen and deuterium there is a substantial deviation in the inferred O-site energy of Fig. 4 once the temperature exceeds about 400 K. We also see that there is a significant difference in what happens at higher temperature in α-phase PdH_x as compared to α-phase PdD_x.

It is hard to imagine some effect cutting in at elevated temperature that would move the O-site energy as would be required to account for the results in Fig. 4. However, if we take the other point of view that the O-site energy changes only on account of the (smooth) change in the Fermi level, then we need to account for the temperature dependence of

the interstitial partition function of Figs. 5 and 6. In both cases one can imagine a scenario in which additional states at low energy would lead to additional contributions to the partition function. This prospect is pursued in Section 3.

3. Model Including Both O-sites and T-sites

Motivated by the discussion of Section 2 we are interested in whether the α-phase solubility data might be consistent with a small or modest amount of tetrahedral site occupation. Whether there should be any T-site occupation at all depends critically on how large the O-site to T-site excitation energy is. The results from embedded atom models, from density functional calculations, and from quantum chemistry calculations range between about 50 meV to about 300 meV. If the excitation energy were as low as 50 meV, then we would expect to see T-site occupation at modest temperature at low loading. On the other hand, if the excitation energy were near 300 meV then we would see very little T-site occupation. The best recent calculations give a low O-site to T-site excitation energy [14–20], and this provides us with motivation to compare model results against experimental data to check for consistency.

We have been interested recently in the development and application of models for both O-site and T-site occupation to understand what happens in PdH and PdD at high loading [13]. With experience gained from the earlier work we are motivated to apply the model to α-phase PdH_x and PdD_x.

3.1. Model for O-site and T-site occupation

From our earlier work on modeling O-site and T-site occupation [13], we can write

$$\mu_D = E_O + \theta_O \frac{\partial E_O}{\partial \theta} + \theta_T \frac{\partial E_T}{\partial \theta} - k_B T \ln \frac{1-\theta_O}{\theta_O} - k_B T \ln z_O, \tag{25}$$

$$\mu_D = E_T + \theta_T \frac{\partial E_T}{\partial \theta} + \theta_O \frac{\partial E_O}{\partial \theta} - k_B T \ln \frac{2-\theta_T}{\theta_T} - k_B T \ln z_T. \tag{26}$$

In the α-phase if the pressure is made sufficiently low the first-order terms can be neglected and the model reduces to

$$E_O \;\rightarrow\; \mu_D + k_B T \ln \frac{1-\theta_O}{\theta_O} + k_B T \ln z_O, \tag{27}$$

$$E_T \;\rightarrow\; \mu_D + k_B T \ln \frac{2-\theta_T}{\theta_T} + k_B T \ln z_T. \tag{28}$$

Since we do not have estimates for θ_O and θ_T separately from experiment, we cannot use these relations directly to determine the O-site and T-site energies. On the other hand it should be possible to estimate E_O and E_T by comparing different versions of the model against experiment to see which provides the best match.

3.2. Partition functions

For the discussion of this section we will make use of the 3D oscillator partition functions described in the previous section for O-site occupation. Similarly, for the T-sites we will use

$$z_T\,[\mathrm{PdH}] = 4\left(\frac{1}{1-\;\mathrm{e}^{-\hbar\omega_T\,[\mathrm{PdH}]/k_B T}}\right)^3, \tag{29}$$

$$z_{\rm T}\ [{\rm PdD}] = 6\left(\frac{1}{1-\ {\rm e}^{-\hbar\omega_{\rm T}\ [{\rm PdD}]/k_{\rm B}T}}\right)^3 \tag{30}$$

and determine values for $\hbar\omega_{\rm T}$ [PdD] and $\hbar\omega_{\rm T}$ [PdH] from optimization.

3.3. Boundary condition at low temperature and ansatz

We have seen that the O-site energy $E_{\rm O}(T)$ temperature dependence is given by the Fermi level shift at low temperature. We will take as an ansatz in our discussion that this also holds at higher temperature; hence

$$E_{\rm O}(T) = E_{\rm O}(0) + \Delta\mu_{\rm F}(T). \tag{31}$$

Since the lattice expands a little as the temperature increases, we might expect that the oscillator energy should decrease. There may be other more subtle effects coming in as well. The idea here is that it may be that these effects altogether are relatively small, and by neglecting them we can focus on T-site occupation. Whether this approach in general is a good one or not will depend ultimately on the results obtained.

3.4. Simple empirical model and optimization

With a specification of the O-site energy, we adopt a similar strategy for the O-site to T-site excitation energy and write

$$\Delta E(T) = \Delta E(0). \tag{32}$$

It would reasonably be expected that terms linear in temperature should not be present in this kind of model, as we would not expect deviations at low temperature from the parts of the model already included. Higher-order terms are simply neglected for this discussion.

This model has three free parameters altogether that can be chosen to minimize a measure of the error given by

$$I = \frac{\displaystyle\sum_{i=1}^{N} w_i \left[\ln\left\{p_i\left(\frac{1-\theta_i}{\theta_i}\right)^2\right\}_{\rm exp} - \ln\left\{p_i\left(\frac{1-\theta_i}{\theta_i}\right)^2\right\}_{\rm model}\right]^2}{\displaystyle\sum_i w_i}. \tag{33}$$

There are many more data points at the lower temperatures, so we have weighted the data points at high temperature higher to compensate.

3.5. Results for α-phase PdD_x

Optimization of the model parameters leads to

$$E_{\rm O}(0) = -\frac{E_{\rm D}}{2} - 70.73\ {\rm meV}, \tag{34}$$

$$\Delta E(0) = 101.81\ {\rm meV}, \tag{35}$$

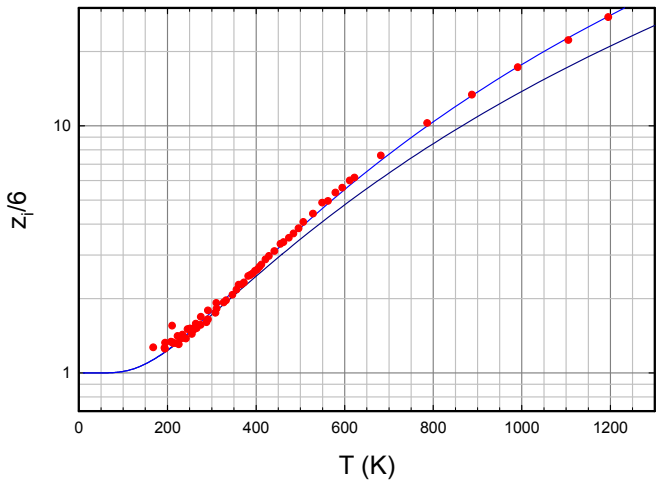

Figure 7. Scaled interstitial partition function versus temperature for α-phase PdD_x; data of Clewley et al. [21] (red circles); 3D oscillator O-site partition function; optimized three-parameter model partition function including O-site and T-site occupation.

$$\hbar\omega_{\rm T}\ [{\rm PdD}] = 66.62\ {\rm meV}. \tag{36}$$

The associated error for this model is

$$I = 0.00480. \tag{37}$$

A comparison of the results for this model and the data of Clewley et al. [21] is shown in Fig. 7. One observes that the model results match well with experiment.

3.6. Input from neutron diffraction experiments

Neutron diffraction experiments seeking tetrahedral occupation in PdD_x were reported by Pitt and Gray [62]. Experiments run at elevated temperature gave positive results for T-site occupation at 309°C. Based on the results given for O-site and T-site occupation separately, the O-site to T-site excitation energy can be determined according to

$$E_{\rm T} - E_{\rm O} = k_{\rm B}T\left\{\ln\left(\frac{2-\theta_{\rm T}}{\theta_{\rm T}}\frac{\theta_{\rm O}}{1-\theta_{\rm O}}\right) + \ln\frac{z_{\rm T}}{z_{\rm O}}\right\}. \tag{38}$$

Results from this analysis are shown in Fig. 8, along with the results from a quadratic least squares fit. The extrapolated value for zero loading is

$$\Delta E(582\ {\rm K}) = 41.6\ {\rm meV}. \tag{39}$$

This value is much lower than the 101.81 meV number obtained from the data of Clewley et al. [21]; both numbers are "low", consistent with the low excitation energies computed in the recent literature, but they do not seem so consistent with each other at this point.

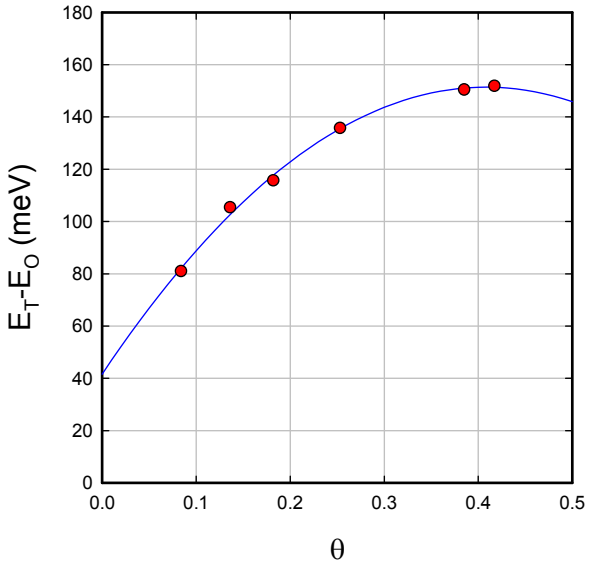

Figure 8. O-site to T-site excitation energy estimated from the neutron diffraction data of Pitt and Gray [62] as a function of loading (red circles); least squares quadratic fit (blue line).

3.7. Result for α-phase PdH_x

A similar optimization for α-phase PdH_x produces

$$E_{\rm O}(0) = -\frac{E_{\rm D}}{2} - 75.09 \text{ meV}, \tag{40}$$

$$\Delta E(0) = 93.24 \text{ meV}, \tag{41}$$

$$\hbar\omega_{\rm T} \text{ [PdH]} = 77.93 \text{ meV}. \tag{42}$$

The error in this case is a bit larger

$$I = 0.00542. \tag{43}$$

A comparison of this fit against the data of Clewley et al. [21] is shown in Fig. 9. The agreement is pretty good.

3.8. Zero-point energy difference

If α-phase PdH_x and α-phase PdD_x were otherwise the same, then we might expect $\Delta E(0)$ to be larger in α-phase PdH_x by the difference in the zero-point energies, which was estimated to be 21.1 meV [13] from the calculations of Ke and Kramer [14]

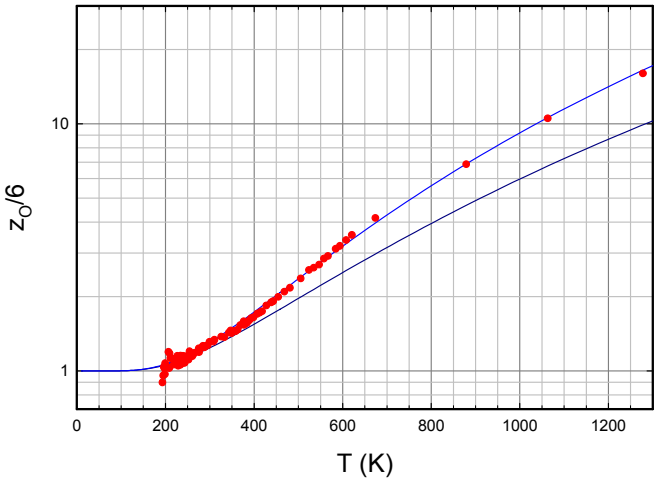

Figure 9. Interstitial partition function versus temperature for α-phase PdH_x; data of Clewley et al. [21] (red circles); 3D oscillator O-site partition function; optimized three-parameter model partition function including O-site and T-site occupation.

$$\left[\Delta E(0)\right]_{\rm PdH} = \left[\Delta E(0)\right]_{\rm PdD} + 21.1 \text{ meV}. \tag{44}$$

The O-site to T-site excitation energies obtained from the optimization of the simple models above are close, but reversed. One would like better agreement, but it would be too much to argue for inconsistency in this case.

3.9. Discussion

We are very much encouraged by the results from optimization of the simple empirical model outlined in this section. Based on the general approach we would expect the model to be most relevant at low temperature; however, the optimizations discussed here are based on global fits over the entire temperature range. The O-site to T-site excitation energies inferred from this analysis are not as close as we might like with results from neutron diffraction measurements, and are reversed relative to what we expect due to zero-point contributions. Neither of these at this point are major inconsistencies.

The model results are shown against $p(1-\theta)^2/\theta^2$ as a function of 1000 K/T in Fig. 10. The results look very good.

4. Improved Empirical Model

Without question there is a some significant success in the application of simple empirical models with both O-site and T-site occupation to the data set of Clewley et al. [21] from the results of Section 3. However, we are motivated to attempt a similar analysis with better models, in the hope of improving consistency with the neutron diffraction data and with the zero-point contribution to the excitation energy. An added benefit is that we will gain some intuition on how sensitive the results are to details of the model used.

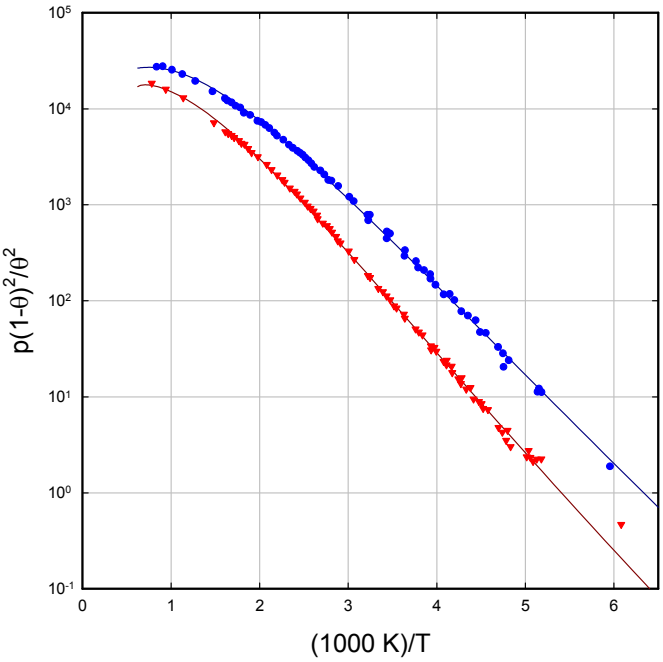

Figure 10. Plot of $p(1-\theta)^2/\theta^2$ for α-phase PdD_x as a function of (1000 K)/T; data set of Clewley et al. [21] for PdH_x (red circles); optimized three-parameter empirical model for PdH_x (red line); data set of Clewley et al. [21] for PdD_x (blue circles); optimized three-parameter empirical model for PdD_x (blue line).

One issue that we might recognize in this discussion is that the excited states as observed from inelastic neutron scattering experiments deviate from those of a three-dimensional harmonic oscillator potential; we can work with a model that is in better agreement with levels that have been observed. We have little guidance from experiment as to what kind of potential we are dealing with for T-site occupation. Due to the relatively low T-site occupation the model is less sensitive to the details. In what follows we will optimize the parameters of the model for the T-site partition function.

4.1. O-site excited state energy levels

The excited state energy levels in PdH from Ross et al. [63] are shown in Fig. 11. Also plotted is a fit based on

$$E_n = \hbar\omega_O n^s \tag{45}$$

with s least squares fit to the data ($s = 1.195$). We include the zero-point energy in the specification of the O-site ground state energy used in the empirical model. This suggests that we might improve the O-site partition function by evaluating it directly with scaled energies

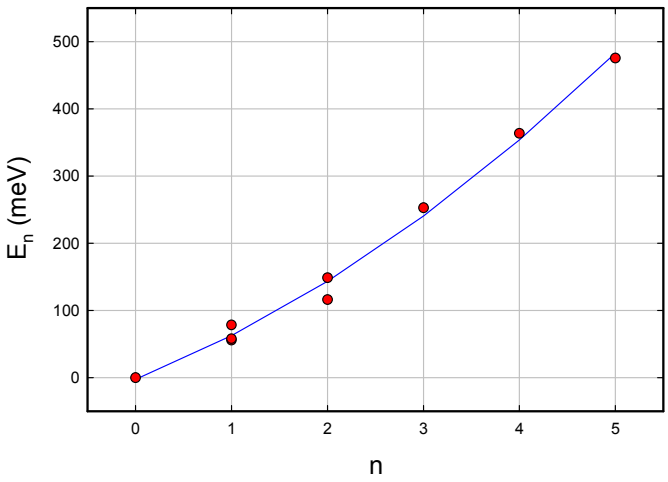

Figure 11. O-site energy levels as a function of the number of quanta for α-phase PdH_x from Ross et al. [63] (red circles); empirical fit (blue line).

$$z_{\rm O}\,[{\rm PdH}] = 2 \times 2 \times \left[\sum_n \exp\left\{ -\frac{E_n}{k_{\rm B}T} \right\} \right]^3 . \tag{46}$$

This approach is one of the simplest possible that includes non-SHO effects. In the models discussed in this section, we have used this approach for the O-site with $s_{\rm O} = 1.2$; for the T-site partition function we will work with different values for $s_{\rm T}$.

4.2. Optimization in the case of α-phase PdD_x

We have optimized a version of the model against the data of Clewley et al. [21] as described in the previous section for different values of $s_{\rm T}$ with the results listed in Table 1. The error is reduced as $s_{\rm T}$ is increased up to a value of 1.636 which is the optimum value if $s_{\rm T}$ is optimized along with the other parameters. We recall that a value of $s = 1$ corresponds to a parabolic potential well in 3D and $s = 2$ corresponds to a square well in 3D; a value of $s = 1.6$ would then imply a T-site well more like a square well than a parabolic well.

Table 1. Fitting parameters for O-site to T-site model for α-phase PdD_x.

$E_{\rm O} + \frac{E_{\rm D}}{2}$ (meV)	$\Delta E(0)$ (meV)	$\hbar\omega_{\rm T}$ [PdD] (meV)	$s_{\rm T}$	I
−70.71	84.9	50.9	1.0	0.00492
−70.90	96.7	39.0	1.2	0.00399
−71.02	107.3	30.1	1.4	0.00361
−71.09	116.7	23.3	1.6	0.00347
−71.10	118.0	22.3	1.636	0.00346

Table 2. Fitting parameters for O-site to T-site model for α-phase PdH_x.

$E_O + \frac{E_D}{2}$ (meV)	$\Delta E(0)$ (meV)	$\hbar\omega_T$ [PdD] (meV)	s_T	I
−75.05	90.4	66.8	1.0	0.00548
−75.21	99.6	53.8	1.2	0.00487
−75.31	108.2	43.7	1.4	0.00464
−75.39	116.1	35.6	1.6	0.00458
−75.39	117.1	34.7	1.627	0.00458

We see that the O-site to T-site excitation energy that produces the best fit with the experimental data increases with the T-site excited state parameter s_T.

4.3. Optimization in the case of α-phase PdH_x

We have optimized a version of the model against the data of Clewley et al. [21] as described in the previous section, with results given in Table 2. One sees a similar trend that the error decreases as s_T increases, this time up to an optimum value of s_T of 1.627.

The excitation energy for PdH_x is seen to increase with s_T similarly to the earlier results for PdD_x.

4.4. Checking consistency with neutron diffraction measurements

We recall that the O-site to T-site excitation energy can be estimated from the neutron diffraction data from

$$E_T - E_O = k_B T \left\{ \ln\left(\frac{2-\theta_T}{\theta_T} \frac{\theta_O}{1-\theta_O} \right) + \ln \frac{z_T}{z_O} \right\}.$$

In our empirical model the excitation energy is assumed independent of temperature, so $E_T - E_O$ here can be compared against our $\Delta E(0)$. The O-site and T-site occupations are given numerically in Pitt and Gray (2002). However, with different models for the O-site and T-site partition functions the ratio of z_T/z_O is now model dependent. In order to check for consistency we need to re-evaluate the excitation energy for the different models. The results are given in Table 3. The empirical model is consistent with the neutron scattering data for $s_T = 1.36$, at an excitation energy of 105.1 meV.

4.5. Results

In the case of α-phase PdD_x we can specify an empirical model which has a lower error than what was found in the previous section, and which is also consistent with the neutron diffraction data. It seems reasonable to assume a similar value for s_T for α-phase PdH_x. The model parameters are listed in Table 4.

Table 3. Comparison of model O-site to T-site excitation energy and excitation energy from neutron diffraction data for different values of s_T.

s_T	model: $\Delta E(0)$ (meV)	data: $E_T - E_O$ (meV)
1.0	84.9	124.1
1.2	96.7	111.7
1.4	107.3	104.0
1.6	116.7	98.9

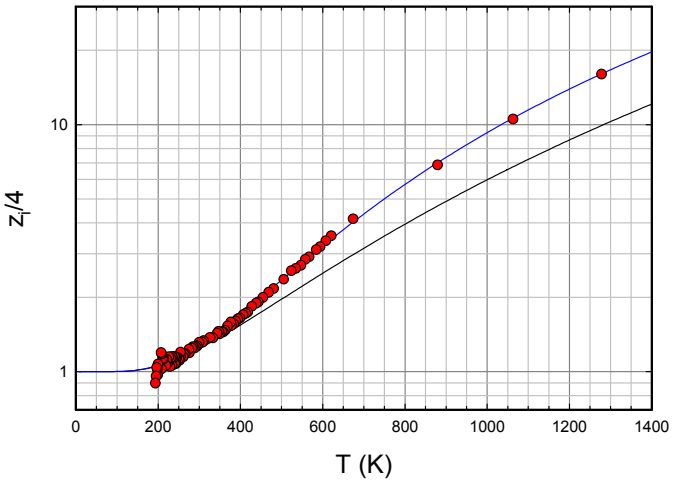

Figure 12. Scaled interstitial partition function versus temperature for α-phase PdH_x; data of Clewley et al. [21] (red circles); 3D oscillator O-site partition function; optimized model partition function including O-site and T-site occupation.

In Figs. 12 and 13 we show the interstitial partition functions for α-phase PdH_x and PdD_x. In both cases the agreement is excellent. In Fig. 14 the data is plotted as in Clewley et al. [21] as $p(1-\theta)^2/\theta^2$ as a function of 1000 K/T; the agreement is again excellent.

In Fig. 15 are shown the O-site and T-site relative occupations

$$\frac{\theta_O}{\theta} = \frac{\theta_O}{\theta_O + \theta_T}, \qquad \frac{\theta_T}{\theta} = \frac{\theta_T}{\theta_O + \theta_T}. \tag{47}$$

The T-site values seem high at elevated temperature; however, if the neutron scattering data of Pitt and Gray [62] are correct, then such high values are needed for consistency. It may be that this data is compromised due to the presence of a substantial number of monovacancies; if so then the T-site occupation would be overestimated. We note that it is straightforward to construct empirical models that fit the data of Clewley et al. [21] very nearly as well that predict a lower T-site occupation. In essence, the data of Clewley et al. [21] seems consistent with substantial T-site occupation, but additional input from experiment is required to determine more precisely how much T-site occupation is present.

5. Discussion and Conclusions

This study was motivated initially by an interest in estimating the O-site to T-site excitation energy at zero loading in order to develop an improved model for PdH and PdD at high loading. We had available a model for both O-site and

Table 4. Fitting parameters for O-site to T-site models for α-phase PdD_x and PdH_x.

	$E_O + \frac{E_D}{2}$ (meV)	$\Delta E(0)$ (meV)	$\hbar\omega_O$ (meV)	s_O	$\hbar\omega_T$(meV)	s_T	I
PdD_x	−71.00	105.3	46.5	1.2	31.6	1.36	0.00366
PdH_x	−75.30	106.5	69.0	1.2	45.5	1.36	0.00467

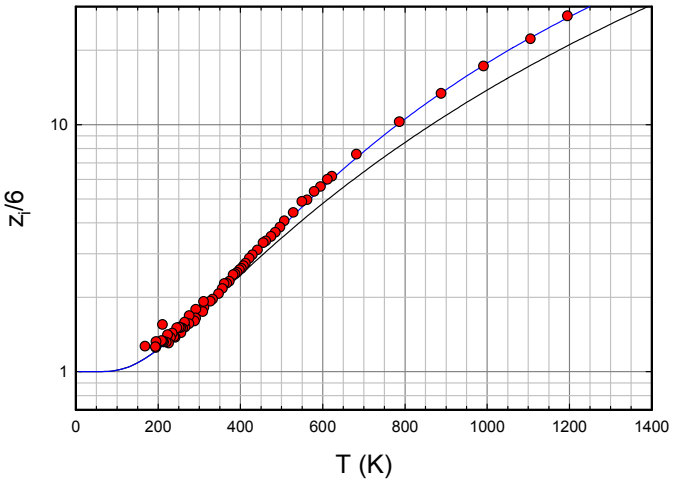

Figure 13. Scaled interstitial partition function versus temperature for α-phase PdD_x; data of Clewley et al. [21] (red circles); 3D oscillator O-site partition function (black line); optimized model partition function including O-site and T-site occupation (blue line).

T-site excitation, one which we had experience with, and also some confidence in. What made this study possible was the data set published be Clewley et al. [21] and an ability to scan it so that we could work with it in digitized form. There was no reason to believe a priori that it would be possible to extract much from the data, other than some evidence either for or against there being signs of T-site occupation.

However, in the course of the study it began to become clear that a model with both O-site and T-site occupation was very relevant to the data, and that interpreting the data based on a model with O-site occupation alone would require some awkward assumptions. We tried a very large number of different approaches an empirical models while studying the problem. A key insight which changed our approach was the recognition that it was possible to account for the approximate linear dependence of the O-site energy at low temperature by the Fermi level shift. With this dominant term included explicitly, it began to emerge that additional corrections were higher order and likely small. This suggested the ansatz that we might be able to understand the system by discarding all temperature dependence other than the Fermi level shift in a model for $E_{\rm O}(T)$.

Once the ansatz was adopted, the data seemed to make sense in terms of relatively simple models. Improving the O-site partition function led to better agreement with the data. We had considered the possibility that all model parameters could be extracted directly from the data in a brute force optimization. It would have been very powerful to have been able to extract the O-site excited state spectrum directly from the data set. Unfortunately there are too many degrees of freedom present, and the overall mathematical optimum leads to a picture that is very much not physically compelling. However, with input from inelastic neutron scattering measurements it was possible to assign solid values to some of the model parameters, and then optimize against the data to determine others.

If we make use of a simple version of the empirical model based on partition functions for 3D harmonic oscillators, then immediately we are able to fit the data well based on physically reasonable model parameters. The O-site and T-site excitation energies that result are 101.81 meV for PdD_x and 93.24 meV for PdH_x. Although there are some minor issues with respect to consistency with neutron diffraction data and the zero-point energy difference, the results

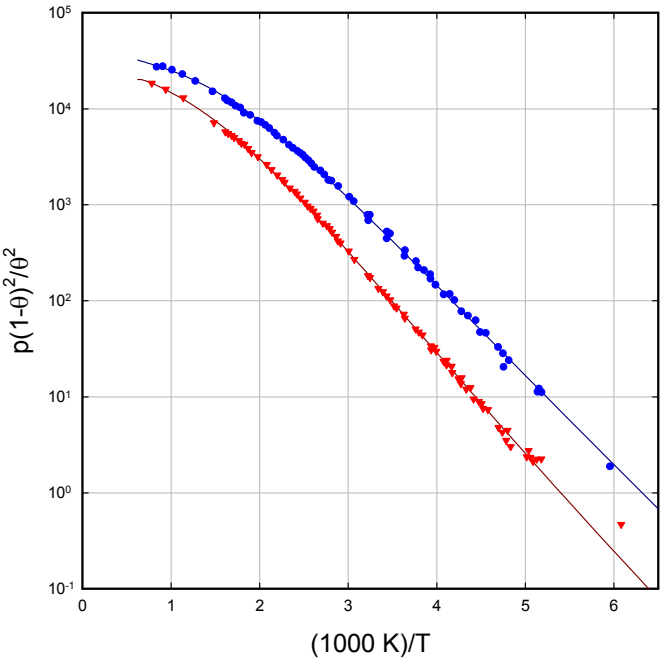

Figure 14. Plot of $p(1-\theta)^2/\theta^2$ for α-phase PdD_x as a function of (1000 K)/T; data set of Clewley et al. [21] for PdH_x (red circles); optimized empirical model for PdH_x (red line); data set of Clewley et al. [21] for PdD_x (blue circles); optimized empirical model for PdD_x (blue line).

are both interesting and probably worth taking seriously. The excitation energies are close to the best numbers from recent theoretical models.

Based on this strong initial result, we were motivated to explore further and see whether it might be possible to extract more from the experimental data set of Clewley et al. [21]. The key issue in this case has to do with the O-site and T-site partition functions. Based on inelastic neutron scattering experiments, we know that the excited state energies of O-site PdH do not scale with energy as a 3D simple harmonic oscillator. Consequently, we might expect to do better if we use a more realistic partition function for the O-sites; as discussed above we end up with smaller errors when we do. We have much less to rely on in the case of the T-site partition function. In this case we can make use of the data set to optimize, and we find a relation between the T-site energy level scaling parameter s_T and the excitation energy. The optimization of s_T in α-phase PdD_x leads to a value of 1.36, which suggests that the T-site is further from being a spherical harmonic oscillator than the O-site. Without analogous input for α-phase PdH_x we adopted the same s_T, even though there is good reason to believe it might be different. Optimization with the resulting non-SHO models leads to estimates for the excitation energy at zero loading of 105.3 meV for PdD_x, and 106.5 meV for PdH_x. We had hoped for a difference in excitation energy between the two cases consistent with the zero-point energy difference (21.1 meV); the energies we found are nearly the same, a result which is compatible with the low prediction based on the zero-point energy.

Perhaps the biggest issue is the substantial T-site occupation fraction, implied by the neutron diffraction data of Pitt

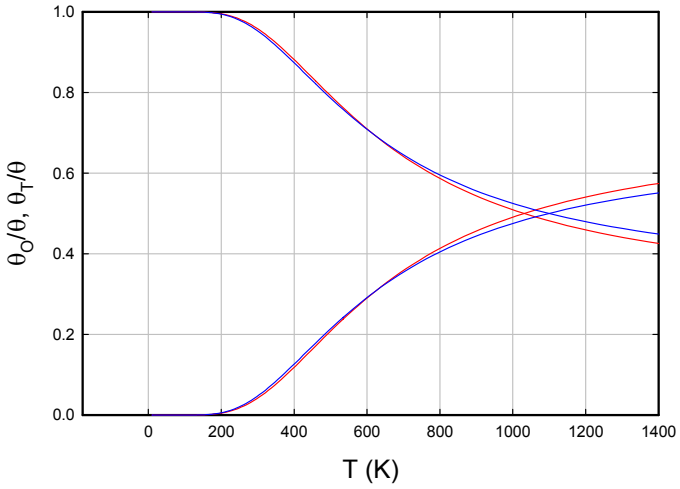

Figure 15. Fractional O-site occupation for α-phase PdH_x (lower red line) and PdD_x (lower blue line), and fractional T-site occupation for α-phase PdH_x (upper red line) and PdD_x (upper blue line).

and Gray [62], and predicted by the empirical models especially at elevated temperature. One should expect significant T-site occupation based on the theoretical estimates from modern structure calculations. However, this is one issue that those familiar with metal hydrides in general, and PdH and PdD in particular, are unlikely to accept without additional confirming experimental data.

The model O-site to T-site excitation energy for α-phase PdD_x depends on what is assumed about the T-site partition function, which is not available at present independently from experiment. If in the future α-phase solubility measurements are done in which the O-site and T-site occupation is determined individually, from the results we would be able to eliminate much uncertainty about excitation energies and partition functions. At present an estimate of 105.3 meV for the excitation energy for α-phase PdD_x seems most consistent with the data we have; but values in the range of 90-110 meV seem possible. The uncertainty is a bit larger for α-phase PdH_x.

Acknowledgments

Assistance from Florian Metzler is acknowledged, who made use of the online digitizer program WebPlotDigitizer of Ankit Rohagti (http://arohatgi.info/WebPlotDigitizer) to digitize the data sets from Clewley et al. [21]. We would like to thank Industrial Heat for support for some of the research reported here.

References

[1] Y. Ebisuzaki and M. O'Keeffe, The solubility of hydrogen in transition metals and alloys, *Progress Solid State Chem.* **4** (1967) 187–211.

[2] E. Wicke, H. Brodowsky and H. Züchner, Hydrogen in palladium and palladium alloys, in *Hydrogen in Metals, Vol. 2*, Springer, Berlin, 1978, pp. 73–155.

[3] W. A. Oates and T. B. Flanagan, The solubility of hydrogen in transition metals and their alloys, *Progress Solid State Chem.* **13** (1981) 193–272.

[4] T.B. Flanagan, Thermodynamics of metal–hydrogen systems, in *Metal Hydrides*, Springer, Berlin, 1981, pp. 361–377.
[5] E. Wicke, Some present and future aspects of metal–hydrogen systems, *Zeitschrift für Physikalische Chemie* **143** (1985) 1–21.
[6] N.A. Gokcen, Interstitial Solutions, in *Statistical Thermodynamics of Alloys*, Springer, Berlin, 1986, pp. 149–193.
[7] L. Schlapbach, *Hydrogen in Intermetallic Compounds I.*, Springer, New York, 1988.
[8] R.Lässer, Properties of protium, deuterium and tritium in selected metals, in *Tritium and Helium-3 in Metals*, Springer, Berlin, 1989, pp. 48–107.
[9] T. B. Flanagan, and W. A. Oates, The palladium–hydrogen system, *Ann. Rev. Materials Sci.* **21** (1991) 269–304.
[10] Y. Fukai, *The Metal–Hydrogen System* Springer, New York, 1991.
[11] F.D. Manchester, A. San-Martin and J.M. Pitre, The H–Pd (hydrogen–palladium) system, *J. phase Equilibria* **15** (1994) 62–83.
[12] J.M. Joubert and S. Thiébaut, Thermodynamic assessment of the Pd-–H-–D-–T system, *J. Nucl. Materials* **395** (2009) 79–88.
[13] P.L. Hagelstein, An empirical model for octahedral and tetrahedral occupation in PdH and in PdD at high loading, *J. Condensed Matter Nucl. Sci.*, (in press).
[14] X. Ke and G.J. Kramer, Absorption and diffusion of hydrogen in palladium–silver alloys by density functional theory, *Phy. Rev. B* **66** (2002) 184304.
[15] P. Kamakoti and D.S. Sholl, A comparison of hydrogen diffusivities in Pd and CuPd alloys using density functional theory, *J. Membrane Sci.* **225** (2003) 145–154.
[16] S.Z. Baykara, Theoretical evaluation of diffusivity of hydrogen in palladium and rhodium, *Int. J. Hydrogen Energy* **29** (2004) 1631–1636.
[17] N. Ozawa, T.A. Roman, H. Nakanishi, H., Kasai, N.B. Arboleda Jr. and W.A. Dino, Potential energy of hydrogen atom motion on Pd (111) surface and in subsurface: A first principles calculation, *J. Appl. Phys.* **101** (2007) 123530.
[18] H, Grönbeck and V.P. Zhdanov, Effect of lattice strain on hydrogen diffusion in Pd: A density functional theory study, *Phy. Rev. B* **84** (2011) 052301.
[19] T.P. Senftle, M.J. Janik and A.C. van Duin, A reaxff investigation of hydride formation in palladium nanoclusters via Monte Carlo and molecular dynamics simulations, *J. Phy. Chem. C* **118** (2014) 4967–4981.
[20] R. Nazarov, T. Hickel and J. Neugebauer, Ab initio study of H-vacancy interactions in fcc metals: Implications for the formation of superabundant vacancies, *Phy. Rev. B* **89** (2014) 144108.
[21] J.D. Clewley, T. Curran, T.B. Flanagan and W.A. Oates, Thermodynamic properties of hydrogen and deuterium dissolved in palladium at low concentrations over a wide temperature range, *J. Chemical Soc., Faraday Trans. 1: Phy. Chem. in Condensed Phases* **69** (1973) 449–458.
[22] R.H. Fowler and C.J. Smithells, A theoretical formula for the solubility of hydrogen in metals, *Proc. Roy. Soc. London. Ser. A, Mathematical and Phy. Sci.* **160** (1937) 37–47.
[23] J.R. Lacher, A theoretical formula for the solubility of hydrogen in palladium, *Proc. Roy. Soc. London. Ser. A, Mathematical and Phy. Sci.* **161** (1937) 525–545.
[24] A. Harasima, T. Tanaka and K. Sakaoku, Cooperative phenomena in Pd–H system I, *J. Phy. Soc. Japan* **3** (1948) 208–213.
[25] T. Tanaka, K. Sakaoku and A. Harasima, Cooperative phenomena in Pd–H system II, *J. Phy. Soc. Japan* **3** (1948) 213–218.
[26] A. L. G. Rees, Statistical mechanics of two-component interstitial solid solutions, *Trans. Faraday Soc.* **50** (1954) 335–342.
[27] R.V. Bucur and M. Crisan, Interprétation mécanique-statistique de l'isotherme de solubilité de l'hydrogène en phase d'hydrure pour les métaux palladium, vanadium, niobium et tantale, *J. Phys. and Chem. of Solids* **28** (1967) 995–1000.
[28] R. Burch, Theoretical aspects of the absorption of hydrogen by palladium and its alloys. Part 1. A reassessment and comparison of the various proton models, *Trans. Faraday Soc.* **66** (1970) 736–748.
[29] T. Hashino and S. Naito, A contribution to the thermodynamics of the interstitial solid solution of hydrogen in metals, *J. Chemical Phys.* **64** (1976) 1016–1021.
[30] H. Ogawa, A statistical-mechanical method to evaluate hydrogen solubility in metal, *J. Phy. Chem. C* **114** (2010) 2134–2143.
[31] V. Tserolas, M. Katagiri, H. Onodera and H. Ogawa, Thermodynamical Modeling of PC Isotherms for Metal Hydride Materials, *Trans. Materials Res. Soc. Japan* **35** (2010) 221–226.
[32] P.O. Orondo, A theoretical model of interstitial hydrogen: pressure-composition-temperature, chemical potential, enthalpy and entropy, MIT Ph.D. Thesis, 2012.
[33] C. Wadell, T. Pingel, E. Olsson, I. Zoric, V.P. Zhdanov and C. Langhammer, Thermodynamics of hydride formation and decomposition in supported sub-10 nm Pd nanoparticles of different sizes, *Chemical Phys. Lett.* **603** (2014) 75–81.

[34] K.A. Moon, Pressure-composition-temperature relations in the palladium–hydrogen system, *J. Phy. Chem.* **60** (1956) 502–504.
[35] D.H. Everett and P. Nordon, Hysteresis in the palladium+hydrogen system, *Proc. Roy. Soc. London A: Mathematical, Phy. and Eng. Sci.* **259** (1960) 341–360.
[36] T.B. Flanagan, Absorption of deuterium by palladium, *J. Phy. Chem.* **65** (1961) 280–284.
[37] J.W. Simons and T.B. Flanagan, Absorption isotherms of hydrogen in the α-Phase of the hydrogen–palladium system, *J. Phy. Chem.* **69** (1965) 3773–3781.
[38] R. Burch and N.B. Francis, N.B. Pressure against composition isotherms and thermodynamic data for the α-phase of the palladium/hydrogen system, *J. Chemical Soc., Faraday Trans. 1: Phy. Chem. in Condensed Phases* **69** (1973) 1978–1982.
[39] T.B. Flanagan and J.F. Lynch, Thermodynamics of a gas in equilibrium with two nonstoichiometric condensed phases. Application to metal/hydrogen systems, *J. Phy. Chem.* **79** (1975) 444–448.
[40] M.J.B. Evans and D.H. Everett, Thermodynamics of the solution of hydrogen and deuterium in palladium, *J. Less Common Metals* **49** (1976) 123–145.
[41] C. Labes and R.B. McLellan, Thermodynamic behavior of dilute palladium–hydrogen solid solutions, *Acta Metallurgica* **26** (1978) 893–899.
[42] C. Picard, O.J. Kleppa and G. Boureau, A thermodynamic study of the palladium–hydrogen system at 245–352^o C and at pressures up to 34 atm, *J. Chemical Phys.* **69** (1978) 5549–5556.
[43] T.B. Flanagan, Enthalpy and entropy changes for non-stoichiometric hydride formation, *J. Less Common Metals* **63** (1979) 209–223.
[44] O.J. Kleppa and R.C. Phutela, A calorimetric-equilibrium study of dilute solutions of hydrogen and deuterium in palladium at 555 to 909 K, *J. Chemical Phys.* **76** (1982) 1106–1110.
[45] R. Lässer and K.H. Klatt, Solubility of hydrogen isotopes in palladium, *Phy. Rev. B* **28** (1983) 748.
[46] R. Lässer, Solubility of protium, deuterium, and tritium in the α phase of palladium, *Phy. Rev. B* **29** (1984) 4765.
[47] R. Lässer and G.L. Powell, Solubility of H, D, and T in Pd at low concentrations, *Phy. Rev. B* **34** (1986) 578.
[48] W.A. Oates, R. Laesser, T. Kuji and T.B. Flanagan, The effect of isotopic substitution on the thermodynamic properties of palladium–hydrogen alloys, *J. Phys. Chem. Solids* **47** (1986) 429–434.
[49] E. Wicke and J. Blaurock, New experiments on and interpretations of hysteresis effects of Pd–D_2 and Pd–H_2, *J. Less Common Metals* **130** (1987) 351–363.
[50] T.B. Flanagan, W. Luo and J.D. Clewley, Calorimetric enthalpies of absorption and desorption of protium and deuterium by palladium, *J. Less Common Metals* **172** (1991) 42–55.
[51] O. Beeri, D Cohen, Z Gavra and M.H. Mintz, The interpretation of hydrogen isotope effects and their relation to microscopic energy related parameters by simplified statistical thermodynamic models, *Physica Scripta* **T94** (2001) 88.
[52] W. Luo, D. Cowgill, R. Causey and K. Stewart, Equilibrium isotope effects in the preparation and isothermal decomposition of ternary hydrides $Pd(H_xD_{1-x})_y$ ($0 < x < 1$ and $y > 0.6$), *The J. Phy. Chem. B* **112** (2008) 8099–8105.
[53] E.A. Crespo, S. Claramonte, M. Ruda and S.R. de Debiaggi, Thermodynamics of hydrogen in Pd nanoparticles, *Int. J. Hydrogen Energy* **35** (2010) 6037–6041.
[54] W. Kolos and L. Wolniewicz, Improved theoretical ground-state energy of the hydrogen molecule, *J. Chemical Phys.* **49** (1968) 404–410.
[55] J.-M. Joubert, A Calphad-type equation of state for hydrogen gas and its application to the assessment of Rh–-H system, *Int. J. Hydrogen Energy* **35** (2010) 2104.
[56] P.L. Hagelstein, S.D. Senturia and T.P. Orlando, *Introductory Applied Quantum and Statistical Mechanics*, Wiley, 1984.
[57] H.C. Urey and D. Rittenberg, Some thermodynamic properties of the H1H2, H2H2 molecules and compounds containing the H2 atom, *J. Chemical Phys.* **1** (1933) 137–143.
[58] C. Elsässer, K.M. Ho, C.T. Chan and M. Fähnle, Vibrational states for hydrogen in palladium, *Phy. Rev. B* **44** (1991) 10377.
[59] F.M. Mueller, A.J. Freeman, J.O. Dimmock and A.M. Furdyna, Electronic structure of palladium, *Phy. Rev. B* **1** (1970) 4617.
[60] F.Y. Fradin, Effect of structure in the electronic density of states on the temperature dependence of the electrical resistivity, *Phy. Rev. Lett.* **33** (1974) 158.
[61] A.B. Sazonov, A.V., Bochkarev and E.P. Magomedbekov, The band structure of solid solutions of hydrogen isotopes in palladium at low temperatures, *Russian J. Phy. Chem. Z. Fizicheskoi Kimii* **78** (2004) 218–224.

[62] M.P. Pitt and E. M. Gray, Tetrahedral occupancy in the Pd–D system observed by in situ neutron powder diffraction, *EuroPhys. Lett.* **64** (2003) 344.

[63] D.K. Ross, V.E. Antonov, E.L. Bokhenkov, A.I. Kolesnikov, E.G. Ponyatovsky and J. Tomkinson, Strong anisotropy in the inelastic neutron scattering from PdH at high energy transfer, *Phy. Rev. B* **58** (1998) 2591.